



Polytopic Linear Models-Based Output Tracking Control of a Single-Link Flexible Joint Robot Manipulator

R. Rajabi, F. Jahangiri*

Department of Electrical Engineering, Shahid Beheshti University, Tehran, Iran.

ABSTRACT: In this paper, to solve the output tracking problem of a single-link flexible joint manipulator, Polytopic Linear Models (PLMs) of the dynamics are made to take advantage of this method. Although linear control methods are very useful due to their powerful theories and simplicity, they can only be used in a neighborhood of the equilibrium point. One way to solve this problem is a PLMs-based method that linearizes the dynamics around several operating points. Therefore, in this paper, after calculating the PLMs of the manipulator, a state feedback control is applied to the derived linear dynamics that are augmented with the dynamics of the output tracking error. An extended method is used to decompose the scheduling space to construct PLMs, which is the segregation method improved with an extra aggregation. In order to avoid creating a large number of local models, an axis-oblique decomposition strategy is used instead of an axis-orthogonal decomposition. In addition, the scheduling functions of the PLMs are determined such that overlaps between the regions are avoided. By this selection, the output tracking problem becomes as a Linear Matrix Inequality (LMI) problem instead of a bilinear matrix inequality problem, which is more difficult to solve and may not lead to an optimal global solution.

Review History:

Received: Feb. 06, 2022

Revised: May, 21, 2022

Accepted: Jul. 17, 2022

Available Online: Oct. 01, 2022

Keywords:

Polytopic Linear Models

Output tracking problem

Axis oblique decomposition

Flexible joint.

1- Introduction

In modern manipulators, flexibility is unavoidable due to the requirements of industrial automation. Flexible links and flexible joints are found in many applications, such as servicing sector, building and maintenance various space stations, gantry cranes, atomic force microscopes, and medical and defense industries [1-3].

Generally, flexibility is an undesirable feature in manipulators since significant control problems like vibrations and deflections are accrued [1, 4-6]. Therefore, the development of control methods for flexible structures has received special attention from researchers [7, 8].

Different control approaches have been discussed to control flexible joint manipulators in literature. The methods such as LQR [9, 10], PID [3, 11], and state feedback [3, 12] are linear model dynamics based control methods. Additionally, adaptive control [13, 14], fuzzy model-based control [15, 16], sliding mode control methods [17-19], and neuro controllers [20, 21] are nonlinear model dynamics-based methods which have been used to control the flexible joint manipulator. Linear systems-based analysis and design methods including controllability, observability, stability analysis, and controller design are well understood and well developed compared to nonlinear systems analysis and design methods. However, the drawback is that the results are just locally valid. Therefore, describing nonlinear dynamical systems by combinations of

linear sub-systems has received significant attention to have a more accurate model. For example, Linear Parameter Varying (LPV) model is used for control purposes, including manipulator control problems [22-24]. However, in this paper we use a simpler method (Polytopic Linear Models (PLMs)) for a flexible joint robot, since in this model the existence of the time-varying parameters complicates the system analysis and controller design. PLMs are built upon a number of linear models introduced by [25]. These linear models describe the system locally within a so-called scheduling regime. Furthermore, even with the existence of uncertainties, the stability of the nonlinear system is guaranteed if its approximated dynamics PLMs is stable [25].

In this paper, PLMs are used to model and control a single-link flexible joint manipulator. In PLMs approximation, scheduling functions determine forms of scheduling regimes. We select them to avoid interference between regions, leading to the tracking control problem becoming an LMI problem rather than a bilinear matrix inequality problem. In addition, to avoid creating many local models, an axis oblique decomposition strategy is used instead of an axis-orthogonal decomposition strategy.

The rest of the paper is organized as follows. Section 2 presents the dynamical model of a single-link flexible manipulator. In section 3, approximation by the PLMs method, including determination of the scheduling regimes and calculating the PLMs parameters, are discussed. Section 4 presents

*Corresponding author's email: fa_jahangiri@sbu.ac.ir



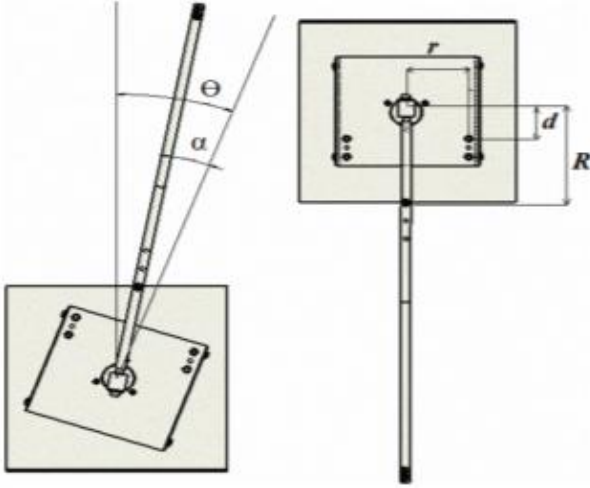


Fig. 1. A single-link flexible joint manipulator [3].

the stability analysis and the method of output tracking control for the flexible joint manipulator. The simulation results demonstrate the effectiveness of the method. Finally, the conclusion of the paper is provided in section 5.

2- Dynamical Model of the Single-Link Flexible Joint Manipulator

Consider the single joint flexible manipulator shown in Fig. 1. The joint mounted on the shaft moves according to the rotation direction of the motor, where θ is the rotation angle of the joint and α , is the oscillation angle of the end effectors.

A mathematical model for this manipulator is obtained from Lagrange equations, as follows [3]:

$$\begin{aligned} \dot{x}_1 &= x_3 \\ \dot{x}_2 &= x_4 \\ \dot{x}_3 &= \frac{K_s}{J_h} x_2 - \frac{K_m^2 K_g^2}{J_h R_m} x_3 + \frac{K_m K_g}{J_h R_m} u \\ \dot{x}_4 &= -\left(\frac{K_s}{J_h} + \frac{K_s}{J_l}\right) x_2 + \frac{K_m^2 K_g^2}{J_h R_m} x_3 + \frac{mgh}{J_l} \sin(x_1 + x_2) - \frac{K_m K_g}{J_h R_m} u \\ y &= x_1 + x_2. \end{aligned} \quad (1)$$

The dynamics consist of four state variables. The first two are $x_1 = \theta$, and $x_2 = \alpha$, the others are their derivations $x_3 = \dot{\theta}$, and $x_4 = \dot{\alpha}$. u is the system input which is the input voltage. The output is the angle of the end effector, which is the sum of the two angles of the rotation angle of the joint θ and the oscillation angle of the link α . The values of the parameters are given in Table 1 [3].

To use the dynamics (1) in a simple form, it is rewritten as follows:

$$\begin{aligned} \dot{x} &= f(x) + bu \\ y &= cx, \end{aligned} \quad (2)$$

where

$$f(x) = \left[x_3, x_4, \frac{K_s}{J_h} x_2 - \frac{K_m^2 K_g^2}{J_h R_m} x_3, -\left(\frac{K_s}{J_h} + \frac{K_s}{J_l}\right) x_2 + \frac{K_m^2 K_g^2}{J_h R_m} x_3 + \frac{mgh}{J_l} \sin(x_1 + x_2) \right]^T,$$

and

$$b = \left[0, 0, \frac{K_m K_g}{J_h R_m}, -\frac{K_m K_g}{J_h R_m} \right]^T,$$

$$c = [1, 1, 0, 0].$$

3- Approximation by PLMs

In this section, an ε -accurate PLMs for the flexible joint manipulator dynamics (1) is derived. The PLMs have the following form [25]:

$$\begin{aligned} \dot{x} &= \sum_{i=1}^N w_i(Z^i) (A_i x + a_i) + bu, \\ y &= cx, \end{aligned} \quad (3)$$

where A_i s and a_i s are the parameters of the PLMs with the size of 4×4 , and 4×1 , respectively. $w_i(Z^i)$ s are the scalar scheduling functions, Z^i is the i^{th} scheduling regime, and N is the number of linear models or scheduling regimes. The approximated model has to be close to the non-linear dynamical model in the sense that they show the same behaviors. One criterion for measuring the accuracy is the Euclidean distance between these two models. The criterion is defined as follows:

$$\text{diff}_{fg}(x) = \sup \left\| f(x) - \sum_{i=1}^N w_i(Z^i) (A_i x + a_i) \right\|_2 \leq \varepsilon, \quad (4)$$

where ε denotes the approximation accuracy.

3- 1- Scheduling Regimes

According to the degree of nonlinearity of the system model, the number of local linear models and their regions forming result in the desired accuracy, should be determined.

In order to reduce the number of linear models or scheduling regimes (denoted by N), the dimension of the scheduling space (denoted by Z) compared to the operating space should be reduced as much as possible since N grows exponentially with Z . The main factor for reducing the dimension of the scheduling space is the existence of some state variables that the dynamical equations are linear with respect to them. In this case, these variables do not participate in the partition-

Table 1. Parameters of the flexible joint manipulator.

Symbol	Description	Value
J_l	Inertia of flexible manipulator	0.003882 Kgm^2
R_m	Motor resistance	15.5 Ω
K_g	Gear ratio of redactor	1/36
K_m	Motor constant	0.0089 $Ns.rad^{-1}$
K_s	Flexibility coefficient of joint	5.468 Nm^{-1}
m	Mass of the flexible joint	0.03235 Kg
g	Gravitational acceleration	-9.81 NKg^{-1}
h	Distance to center of gravity of rotational platform of flexible manipulator	0.06 m
J_h	Inertia of rotational platform	0.00035 Kgm^2

ing, since the approximation of the relevant terms becomes themselves by any partitioning. For the flexible joint manipulator dynamics (1), all terms of the first, second, and third equations are linear with respect to the state variables and the input. For the fourth equation, the term $\sin(x_1 + x_2)$ is non-linear, and therefore it is enough to partition only this term for partitioning the scheduling space of the system (1). Afterwards, parameters of the following approximation should be calculated for every region:

$$\sin(x_1 + x_2) \cong \sum_{i=1}^N w_i(Z^i) (\alpha_i x_1 + \beta_i x_2 + \lambda_i), \quad (5)$$

where α_i and β_i are the entries of the fourth row, the columns one and two in the matrix A_i , respectively. λ_i is the fourth element of the vector a_i .

To decompose the scheduling space Z in N disjoint regions Z^i s, various procedures like uniform decomposition, aggregation, segregation, and extended method that is segregation with an extra aggregation are used [25]. The methods

should be applied such that ε -accuracy is achieved. In addition, there are two major strategies for partitioning the scheduling space: an axis-orthogonal partitioning strategy [25] and an axis-oblique partitioning strategy [26]. The advantages of the first strategy include efficient structure and using parameters learning schemes such as LOLIMOT (local linear model tree). However, the axis-orthogonal partitioning restricts the model flexibility. The second strategy, an axis oblique decomposition strategy, grasps the character of the nonlinearity and therefore requires significantly less number of linear models. This paper reduces the number of models N , using the extended method with an axis-oblique decomposition strategy instead of the axis-orthogonal decomposition strategy.

To approximate $\sin(x_1 + x_2)$, we define a variable as follows for simplicity and to avoid creating a large number of hyper cubes and then partition $\sin(\psi)$ with respect to this new variable:

$$\psi \triangleq x_1 + x_2, \quad (6)$$

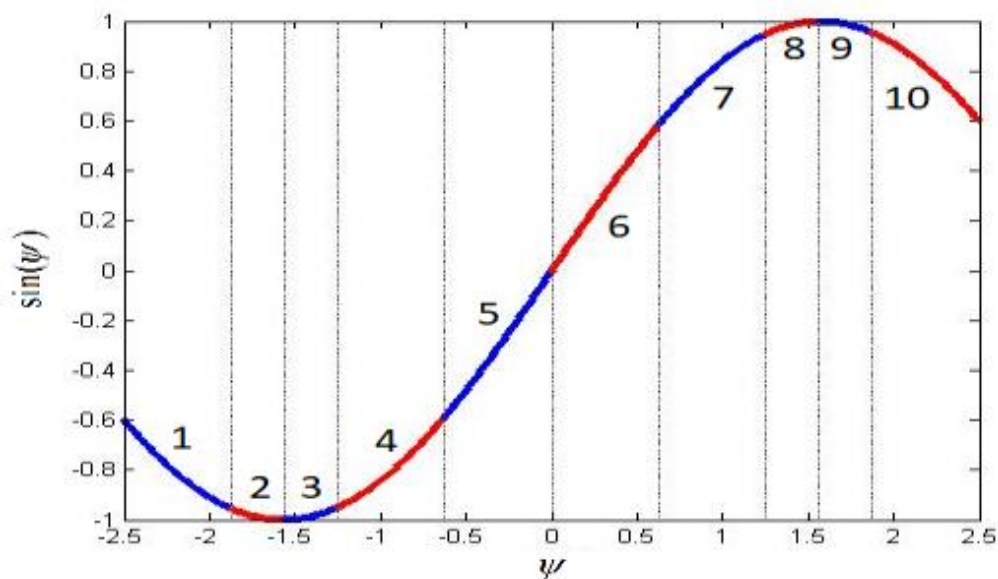


Fig. 2. Partitioning $\sin(\psi)$ by segregation method.

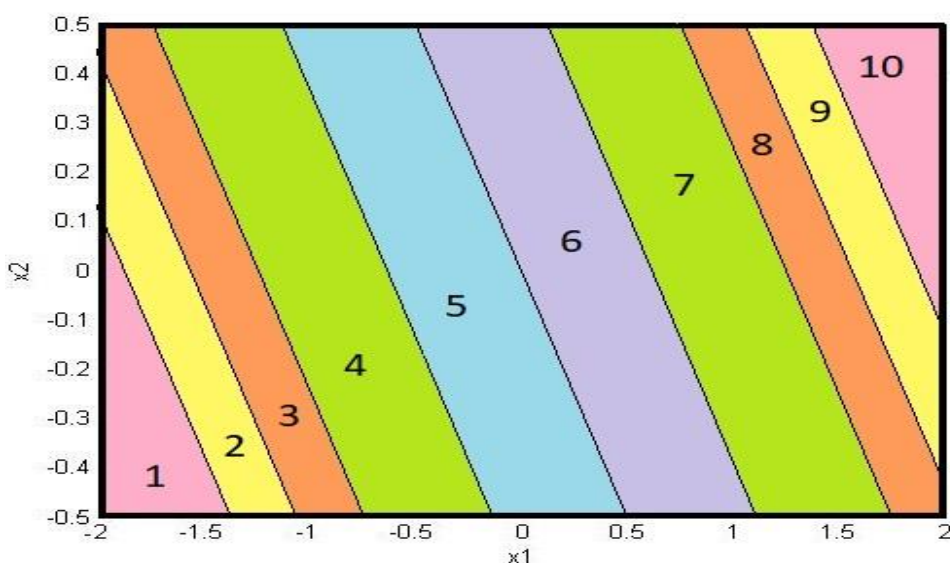


Fig. 3. Segregation regions of $\sin(\psi)$ versus the corresponding values x_1 and x_2 .

Due to the scheduling space of the flexible joint manipulator, $|x_1| \leq 2$, and $|x_2| \leq 0.5$ are considered, which result in $|\psi| \leq 2.5$. To partition $\sin(\psi)$ by the extended method for the segregation step, first we start with the most simple PLMs that consist of a single linear model that covers the entire scheduling space, $|\psi| \leq 2.5$. Obviously, this linear model is not an accurate description of $\sin(\psi)$ unless around the origin. Therefore, we split two sides of the scheduling space into two scheduling regimes, $|\psi \pm 1.25| \leq 1.25$. We once again observe that this segregation is not an accurate description of the function, and it needs more regions. Fig. 2 is obtained

by continuing this approach until having the accuracy of $\varepsilon = 0.1$. By an axis-oblique decomposition strategy and using equation (6), the obtained regions according to x_1 and x_2 would be as Fig. 3. The upper and lower bounds of each region are given in Table 2.

In addition, for simplicity and having less number of regions with the desired accuracy, the scheduling regions can be reduced to seven regions using extra aggregation. For this purpose, the aggregation of neighboring regions was examined, and were aggregated for the cases with maintained desired accuracy. Therefore, Fig. 4 partitioning is obtained for

Table 2. The upper and lower bounds of ψ after partitioning by segregation method.

Region No.	Bounds	Region No.	Bounds
1	[-2.5000,-1.8750]	6	[+0.0000,+0.6250]
2	[-1.8750,-1.5625]	7	[+0.6250,+1.2500]
3	[-1.5625,-1.2500]	8	[+1.2500,+1.5625]
4	[-1.2500,-0.6250]	9	[+1.5625,+1.8750]
5	[-0.6250,-0.0000]	10	[+1.8750,+2.5000]

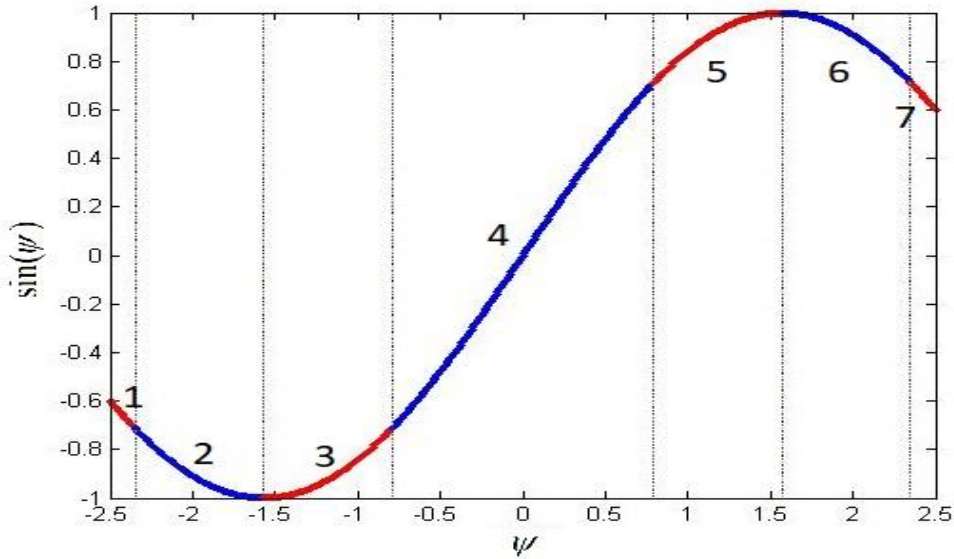


Fig. 4. Partitioning $\sin(\psi)$ by segregation with extra aggregation.

$\sin(\psi)$. The corresponding regions are shown in Fig. 5. The upper and lower bounds of each region are given in Table 3.

3- 2- Scheduling Parameters

After decomposing the scheduling space Z in N disjoint regions Z^i s, the value of the PLMs parameters (3) consisting of two categories (the set of linear models $\{A_i, a_i\}$ s and the scheduling functions $w_i(Z^i)$ s) should be determined. For a flexible joint manipulator, the number of these parameters reduce as mentioned in (5). They are calculated by linearization of the nonlinear system (2) at the centers of the scheduling regimes z_0^i s for the first category $\{A_i, a_i\}$ s , as follows:

$$A_i = \frac{\partial f}{\partial x} \Big|_{z_0^i}, \quad a_i = f(x) \Big|_{z_0^i} - A_i x; \quad i = 1, 2, \dots, N. \quad (7)$$

For every region of Table 3, the calculated parameters are given in Table 4.

For the second category, the scheduling functions should be determined such that the following properties are satisfied [25]:

$$w_i(Z^i) \geq 0, \quad \sum_{i=1}^N w_i(Z^i) = 1. \quad (8)$$

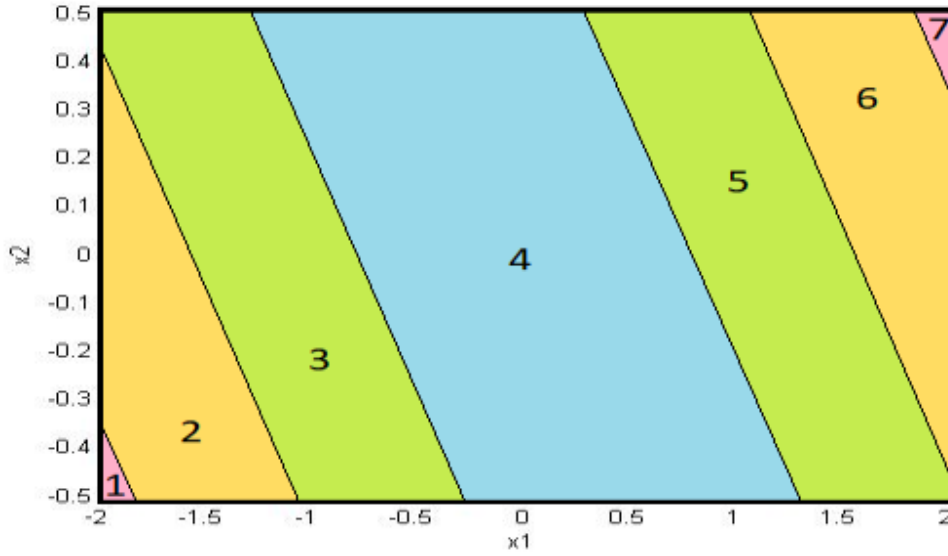


Fig. 5. The segregation with extra aggregation regions of $\sin(\psi)$ versus the corresponding x_1 and x_2 .

Table 3. The upper and lower bounds of ψ after extra aggregation.

Region No.	Bounds	Region No.	Bounds
1	[-2.5,-2.35]	5	[0.79,1.57]
2	[-2.35,-1.57]	6	[1.57,2.35]
3	[-1.57,-0.79]	7	[2.35,2.5]
4	[-0.79,0.79]		

Different selections of $w_i(Z^i)$ s result in different PLMs. If the scheduling functions are selected such that there are overlaps between the regions, the controller design needs to solve a bilinear matrix inequality. Therefore, solving the problem will be much more complex and time-consuming, in addition to the fact that existing methods for solving bilinear matrix inequalities will not necessarily lead to a globally optimal solution. In this paper, to avoid overlaps between the regions, the scheduling functions are defined as follows:

$$w_i(Z^i) = \begin{cases} 1 & (x_1, x_2) \in Z^i \\ 0 & (x_1, x_2) \notin Z^i \end{cases} \quad (9)$$

Using (9) and the parameters given in Table 4 in (5), an approximation of the function $\sin(x_1 + x_2)$ is obtained, as shown in Fig. 6. The difference between these two functions is shown in Fig. 7. It is observed that the maximum value of the differences in the scheduling space is less than 0.1. Using the approximation of this nonlinear term, the PLMs approximation of the whole system (1) is determined easily.

4- Output Tracking Control

In this section, we design a controller for the output tracking problem of the flexible joint manipulator. To this end, we use the results of a theorem that is given as follows.

Consider a nonlinear dynamical system and its approximation PLMs as follows:

Table 4. The first category of the parameters for every scheduling regime.

i	(x_{10}^i, x_{20}^i)	α_i	β_i	λ_i
1	(-1.940,-0.485)	-0.7540	-0.7540	-2.4854
2	(-1.568,-0.392)	-0.3795	-0.3795	-1.6689
3	(-0.944,-0.236)	+0.3809	+0.3809	-0.4751
4	(0,0)	+1	+1	0
5	(+0.944,+0.236)	+0.3809	+0.3809	+0.4751
6	(+1.568,+0.392)	-0.3795	-0.3795	+1.6689
7	(+1.940,+0.485)	-0.7540	-0.7540	+2.4854

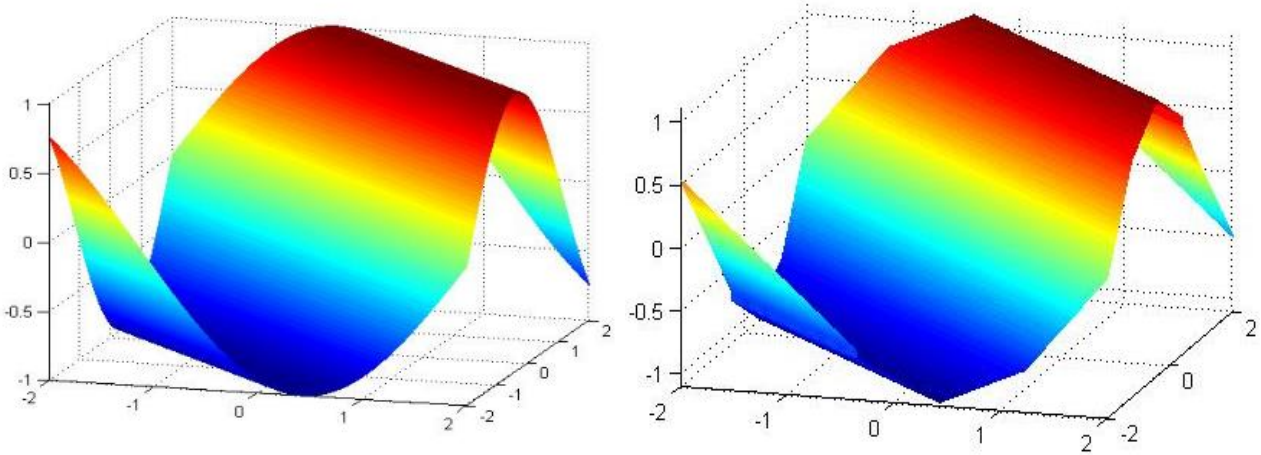


Fig. 6. $\sin(x_1 + x_2)$ (left-side) and its approximation PLMs (right-side).

$$\dot{x} = f(x), \tag{10}$$

$$\dot{x} = \sum_{i=1}^N w_i(Z^i)(A_i x + a_i). \tag{11}$$

It is assumed that, $f(\cdot)$ is a sufficiently smooth function. It has been proved that the mismatch between the system and PLMs is bounded by $\|F_i(x)\|_2 \leq L_i \|x - x_0^i\|_2$, and $L_i \|x - x_0^i\|_2 \leq \epsilon^2$, where, L_i is a finite positive number and $F_i(x)$ is the Taylor expansion remainder of $f(x)$ at the center point x_0^i . For stability of both systems, the following theorem holds:

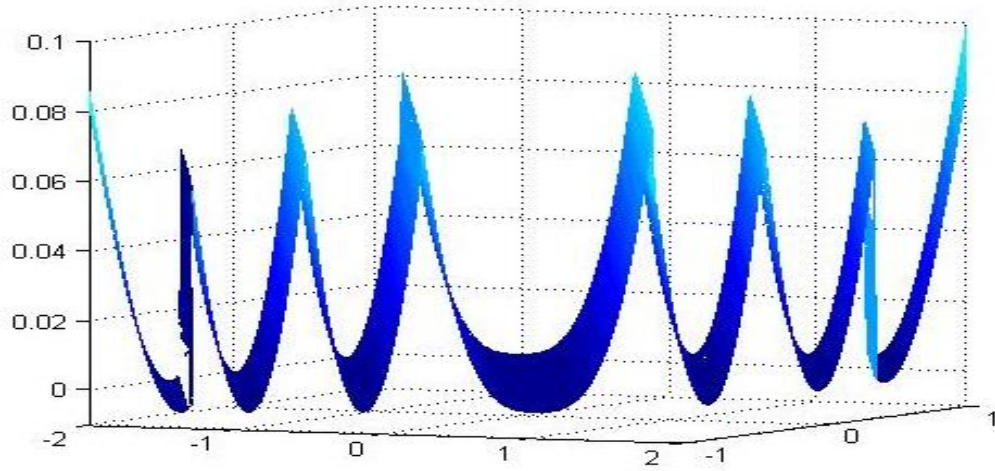


Fig. 7. Difference between $\sin(x_1 + x_2)$ and its approximation PLMs.

$$\begin{pmatrix} A_i^T P + PA_i + L_i \tau_{i1} I & P \\ P & -\tau_{i1} I \end{pmatrix} < 0; \\ \text{if } L_i x_0^{iT} x_0^i \leq \varepsilon^2,$$

$$\begin{pmatrix} A_i^T P + PA_i + L_i(\tau_{i1} - \tau_{i2})I & P & Pa_i + L_i x_0^i(\tau_{i2} - \tau_{i1}) \\ P & -\tau_{i1} I & 0 \\ a_i^T P + L_i x_0^{iT}(\tau_{i2} - \tau_{i1}) & 0 & L_i x_0^{iT} x_0^i(\tau_{i1} - \tau_{i2}) + \varepsilon^2 \tau_{i2} \end{pmatrix} < 0; \\ \text{if } L_i x_0^{iT} x_0^i > \varepsilon^2. \quad (12)$$

Theorem 1 [25]: The nonlinear dynamics (10) and its ε -accuracy approximation PLMs (11) are asymptotically stable, if there exist a matrix $P = P^T > 0$, and scalars $\tau_{ij} \geq 0$ with $i \in \{1, \dots, N\}$ and $j \in \{1, 2\}$, such that the following inequalities hold:

We define a new dynamic for output tracking control of the flexible joint manipulator, as follows:

$$\dot{q} \triangleq r(t) - y(t). \quad (13)$$

where $r(t)$ is the reference signal. Therefore, using (2) and (13), the augmented state space equations of the flexible joint manipulator will be as follows:

$$\begin{aligned} \dot{x} &= \sum_{i=1}^N w_i(Z^i) \{A_i x + b u + a_i\}, \\ \dot{q} &= r - c x. \end{aligned} \quad (14)$$

Now, using the state feedback control as:

$$u(t) = \sum_{i=1}^N w_i(Z^i) u_i(t); \quad u_i(t) = \begin{bmatrix} -k_i & -m_i \end{bmatrix} \begin{bmatrix} x \\ q \end{bmatrix} - \sigma_i, \quad (15)$$

where k_i , m_i , and σ_i are the controller parameters, the closed-loop system becomes:

$$\begin{aligned} \dot{x} &= \sum_{i=1}^N w_i(Z^i) \{A_i x + b \sum_{j=1}^N w_j(Z^j) (-k_j x - m_j q - \sigma_j) + a_i\} \\ \dot{q} &= r - c x. \end{aligned} \quad (16)$$

Using $\sum_{j=1}^N w_j(Z^j) = 1$ from (8), equation (16) is rewritten as follows:

$$\begin{aligned} \dot{x} &= \sum_{i=1}^N w_i(Z^i) \{ \sum_{j=1}^N w_j(Z^j) A_i x + b \sum_{j=1}^N w_j(Z^j) (-k_j x - m_j q - \sigma_j) + \sum_{j=1}^N w_j(Z^j) a_i \} \\ &= \sum_{i=1}^N \sum_{j=1}^N w_i(Z^i) w_j(Z^j) \{ (A_i - b k_j) x - b m_j q + (a_i - b \sigma_j) \}, \\ \dot{q} &= r - c x. \end{aligned} \quad (17)$$

It is simplified to:

$$\begin{aligned} \dot{x} &= \sum_{i=1}^N w_i(Z^i) \{ (A_i - b k_i) x - b m_i q + (a_i - b \sigma_i) \} \\ \dot{q} &= r - c x, \end{aligned} \quad (18)$$

By selecting the scheduling functions as (9), results in:

$$w_i(Z^i)w_j(Z^j) = \begin{cases} w_i(Z^i) & i = j \\ 0 & i \neq j \end{cases} \quad (19)$$

Therefore, (18) can be written as:

$$\begin{bmatrix} \dot{x} \\ \dot{q} \end{bmatrix} = \sum_{i=1}^N w_i(Z^i) \left\{ \begin{bmatrix} A_i & 0_{4 \times 4} \\ -c & 0_{1 \times 1} \end{bmatrix} \begin{bmatrix} b \\ 0_{1 \times 1} \end{bmatrix} \begin{bmatrix} k_i & m_i \end{bmatrix} \begin{bmatrix} x \\ q \end{bmatrix} + \begin{bmatrix} a_i \\ r \end{bmatrix} - \begin{bmatrix} b \\ 0_{1 \times 1} \end{bmatrix} \sigma_i \right\}, \quad (20)$$

which is rewritten as:

$$\begin{bmatrix} \dot{x} \\ \dot{q} \end{bmatrix} = \sum_{i=1}^N w_i(Z^i) \{ (\bar{A}_i - \bar{b} \bar{k}_i) \begin{bmatrix} x \\ q \end{bmatrix} + (\bar{a}_i - \bar{b} \bar{\sigma}_i) \}, \quad (21)$$

By defining following vectors and matrices, we have:

$$\bar{A}_i \triangleq \begin{bmatrix} A_i & 0_{4 \times 4} \\ -c & 0_{1 \times 1} \end{bmatrix}, \quad \bar{b} \triangleq \begin{bmatrix} b \\ 0_{1 \times 1} \end{bmatrix}, \quad \bar{k}_i \triangleq [k_i \quad m_i], \quad \bar{a}_i \triangleq \begin{bmatrix} a_i \\ r \end{bmatrix}, \quad (22)$$

$$\bar{\sigma}_i \triangleq \sigma_i.$$

Equation (21) is described by:

$$\dot{\bar{x}} = \sum_{i=1}^N w_i(Z^i) \{ G_i \bar{x} + \eta_i \}, \quad (23)$$

using the following definitions:

$$\bar{x} \triangleq \begin{bmatrix} x \\ q \end{bmatrix}, \quad G_i \triangleq \bar{A}_i - \bar{b} \bar{k}_i, \quad \eta_i \triangleq \bar{a}_i - \bar{b} \bar{\sigma}_i. \quad (24)$$

It is seen that (23) has the same form as the dynamical equation (11). Therefore, from Theorem 1, asymptotic stability of the closed-loop system (21) is guaranteed if the following conditions hold:

$$\begin{aligned} & \begin{pmatrix} G_i^T P + P G_i + L_i \tau_{i1} I & P \\ P & -\tau_{i1} I \end{pmatrix} < 0; \\ & \text{if } L_i \bar{x}_0^{iT} \bar{x}_0^i \leq \varepsilon^2, \\ & \begin{pmatrix} G_i^T P + P G_i + L_i (\tau_{i1} - \tau_{i2}) I & P & P \eta_i + L_i \bar{x}_0^i (\tau_{i2} - \tau_{i1}) \\ P & -\tau_{i1} I & 0 \\ \eta_i^T P + L_i \bar{x}_0^{iT} (\tau_{i2} - \tau_{i1}) & 0 & L_i \bar{x}_0^{iT} \bar{x}_0^i (\tau_{i1} - \tau_{i2}) + \varepsilon^2 \tau_{i2} \end{pmatrix} < 0; \\ & \text{if } L_i \bar{x}_0^{iT} \bar{x}_0^i > \varepsilon^2, \end{aligned} \quad (25)$$

or equivalently:

$$\begin{aligned} & \begin{pmatrix} (\bar{A}_i - \bar{b} \bar{k}_i)^T P + P (\bar{A}_i - \bar{b} \bar{k}_i) + L_i \tau_{i1} I & P \\ P & -\tau_{i1} I \end{pmatrix} < 0; \\ & \forall L_i \bar{x}_0^{iT} \bar{x}_0^i \leq \varepsilon^2, \\ & \begin{pmatrix} (\bar{A}_i - \bar{b} \bar{k}_i)^T P + P (\bar{A}_i - \bar{b} \bar{k}_i) + L_i (\tau_{i1} - \tau_{i2}) I & P & P (\bar{a}_i - \bar{b} \bar{\sigma}_i) + L_i \bar{x}_0^i (\tau_{i2} - \tau_{i1}) \\ P & -\tau_{i1} I & 0 \\ (\bar{a}_i - \bar{b} \bar{\sigma}_i)^T P + L_i \bar{x}_0^{iT} (\tau_{i2} - \tau_{i1}) & 0 & L_i \bar{x}_0^{iT} \bar{x}_0^i (\tau_{i1} - \tau_{i2}) + \varepsilon^2 \tau_{i2} \end{pmatrix} < 0; \\ & \forall L_i \bar{x}_0^{iT} \bar{x}_0^i > \varepsilon^2. \end{aligned} \quad (26)$$

Defining new variables as follows:

$$P \bar{b} \bar{\sigma}_i \triangleq \mu_i, \quad P \bar{b} \bar{k}_i \triangleq Y_i, \quad (27)$$

The conditions (26) become as linear matrix inequalities:

$$\begin{aligned} & \begin{pmatrix} \bar{A}_i^T P + P \bar{A}_i - (Y_i + Y_i^T) + L_i \tau_{i1} I & P \\ P & -\tau_{i1} I \end{pmatrix} < 0; \\ & \forall L_i \bar{x}_0^{iT} \bar{x}_0^i \leq \varepsilon^2, \\ & \begin{pmatrix} \bar{A}_i^T P + P \bar{A}_i - (Y_i + Y_i^T) + L_i \tau_{i1} I - L_i \tau_{i2} I & P & P \bar{a}_i - \mu_i + L_i \bar{x}_0^i \tau_{i2} - L_i \bar{x}_0^i \tau_{i1} \\ P & -\tau_{i1} I & 0 \\ \bar{a}_i^T P - \mu_i^T + L_i \bar{x}_0^{iT} \tau_{i2} - L_i \bar{x}_0^{iT} \tau_{i1} & 0 & L_i \bar{x}_0^{iT} \bar{x}_0^i \tau_{i1} - L_i \bar{x}_0^{iT} \bar{x}_0^i \tau_{i2} + \varepsilon^2 \tau_{i2} \end{pmatrix} < 0; \\ & \forall L_i \bar{x}_0^{iT} \bar{x}_0^i > \varepsilon^2. \end{aligned} \quad (28)$$

Solving (28) for P , μ_i , and Y_i , and substituting them into (27), the controller parameters, $\bar{k}_i = [k_i, m_i]$ and $\bar{\sigma}_i = \sigma_i$ are obtained. These parameters were obtained for the flexible joint manipulator, as given in Table 5.

Applying the controller to the nonlinear system (1), it is seen that the output $y = \theta + \alpha$, tracks the reference signal well, which is shown in Fig. 8. The reference signal has been considered as a combination of functions such as step, ramp, and sinusoidal in all operating spaces of the system, to test the performance of the controller in the various regions. As a comparison, we also used state feedback control in a single linear model that the tracking result of which is also shown in Figure 8. It is observed that better tracking is achieved using PLMs due to linearization around several operating points that lead to a better approximation of the model compared to the linearized model around only one operating point. In a single linear model, the greater the distance from the operating point, the greater the error. Furthermore, Fig. 9 shows the control signal for the PLMs method. As seen in Fig. 10, a good approximation is achieved for the state variables of the nonlinear system and its approximated system PLMs using the same control signal.

Table 5. Controller parameters.

i	k_{1i}	k_{2i}	k_{3i}	k_{4i}	m_i	σ_i
1	-0.0055	+3.1230	+13.4750	-13.9163	-10.5281	0
2	+0.0006	+3.1235	+13.4819	-13.9244	-13.1601	0
3	+0.0117	+3.1251	+13.4952	-13.9403	-10.9050	0
4	+0.0196	+3.1288	+13.5077	-13.9557	-11.1588	0
5	+0.0117	+3.1251	+13.4952	-13.9403	-10.9050	0
6	+0.0006	+3.1235	+13.4819	-13.9244	-13.1601	0
7	-0.0055	+3.1230	+13.4750	-13.9163	-10.5281	0

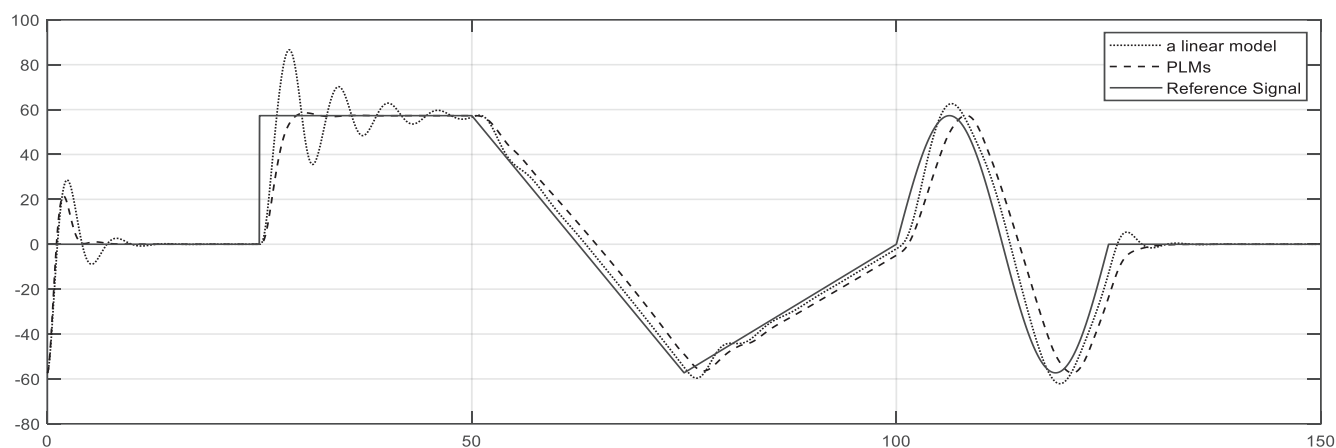


Fig. 8. The output tracking by two modeling methods; PLMs and a linear model.

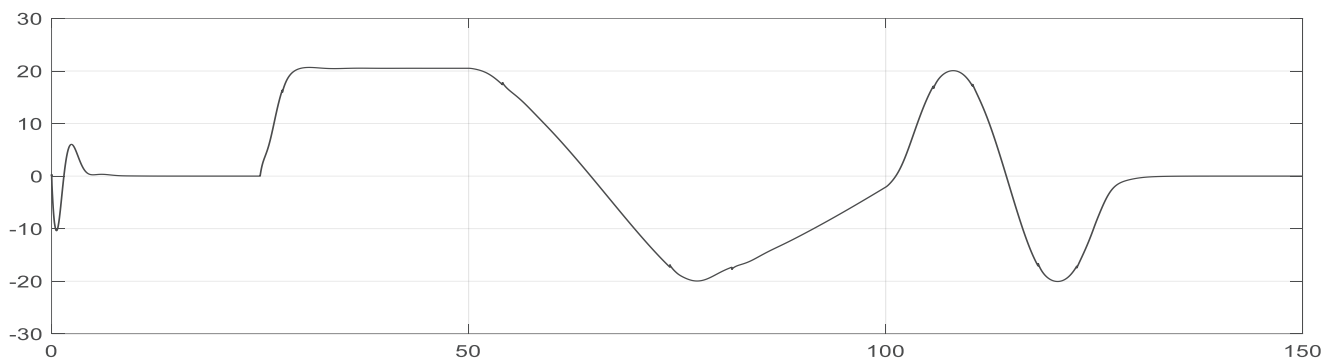


Fig. 9. Control signal.

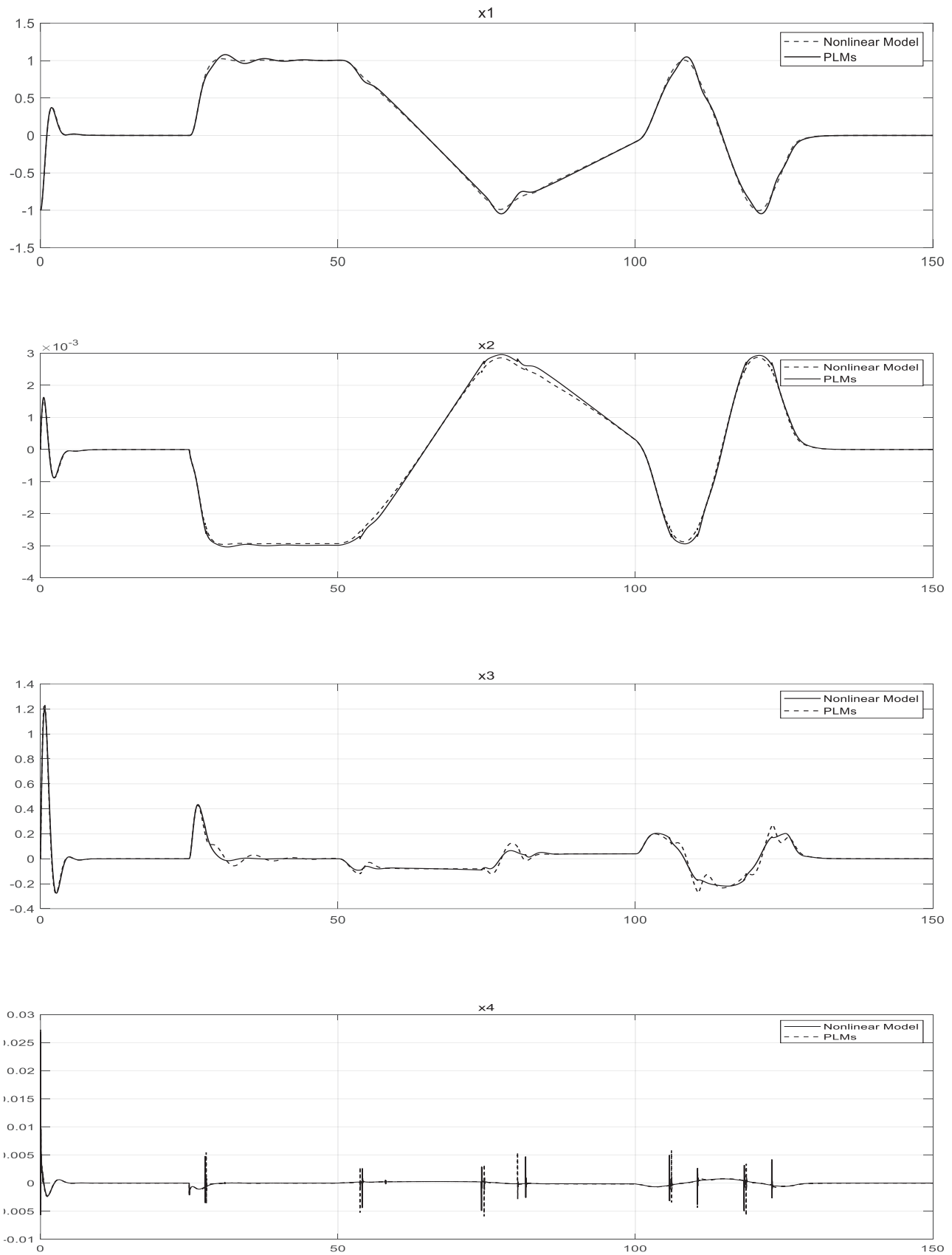


Fig. 10. State variables of the nonlinear system and its PLMs approximation.

5- Conclusion

This study has investigated the output tracking control problem of a single-link flexible joint manipulator. Due to the existence of powerful tools in linear control theory, the PLMs based methods were applied for modeling and controlling the flexible joint manipulator. In order to decrease the number of local models and to avoid the curse of dimensionality, an axis oblique decomposition was used for the partitioning purpose. To determine the parameters of each region, the scheduling functions were selected such that the interference between the regions and therefore requiring to solve bilinear matrix inequality were avoided. Hence, by solving an LMI, the controller was designed and applied to the flexible dynamics.

References

- [1] D. Meng, Y. She, W. Xu, W. Lu, and B. Liang, "Dynamic modeling and vibration characteristics analysis of flexible-link and flexible-joint space manipulator," *Multibody System Dynamics*, vol. 43, no. 4, pp. 321-347, 2018.
- [2] M. A. Mabrok, "New results on negative imaginary systems theory with application to flexible structures and nano-positioning," Australian Defence Force Academy, 2013.
- [3] I. H. Akyuz, E. Yolacan, H. M. Ertunc, and Z. Bingul, "PID and state feedback control of a single-link flexible joint robot manipulator," in *IEEE International Conference on Mechatronics*, 2011, pp. 409-414.
- [4] Y. Li, S. S. Ge, Q. Wei, T. Gan, and X. Tao, "An online trajectory planning method of a flexible-link manipulator aiming at vibration suppression," *IEEE Access*, vol. 8, pp. 130616-130632, 2020.
- [5] O. A. Garcia-Perez, G. Silva-Navarro, and J. F. Peza-Solis, "Flexible-link robots with combined trajectory tracking and vibration control," *Applied Mathematical Modelling*, vol. 70, pp. 285-298, 2019.
- [6] L. Sun, W. Yin, M. Wang, and J. Liu, "Position control for flexible joint robot based on online gravity compensation with vibration suppression," *IEEE Transactions on Industrial Electronics*, vol. 65, no. 6, pp. 4840-4848, 2017.
- [7] D. Subedi, I. Tyapin, and G. Hovland, "Review on modeling and control of flexible link manipulators," *Modeling, Identification and Control*, vol. 41, no. 3, pp. 141-163, 2021.
- [8] S. Ozgoli and H. Taghirad, "A survey on the control of flexible joint robots," *Asian Journal of Control*, vol. 8, no. 4, pp. 332-344, 2006.
- [9] O. Khan, M. Pervaiz, E. Ahmad, and J. Iqbal, "On the derivation of novel model and sophisticated control of flexible joint manipulator," *Revue Roumaine des Sciences Techniques - Serie Électrotechnique et Énergétique*, vol. 62, pp. 103-108, 2017.
- [10] N. Razmjoooy, M. Ramezani, and A. Namadchian, "A new LQR optimal control for a single-link flexible joint robot manipulator based on grey wolf optimizer," vol. 10, p. 53, 2016.
- [11] K. Ibrahim and A. B. Sharkawy, "A hybrid PID control scheme for flexible joint manipulators and a comparison with sliding mode control," *Ain Shams Engineering Journal*, vol. 9, no. 4, pp. 3451-3457, 2018.
- [12] L. L. Tien, A. A. Schaffer, and G. Hirzinger, "MIMO state feedback controller for a flexible joint robot with strong joint coupling," in *IEEE International Conference on Robotics and Automation*, 2007, pp. 3824-3830.
- [13] K. Khorasani, "Adaptive control of flexible joint robots," in *IEEE International Conference on Robotics and Automation*, 1991, pp. 2127-2134.
- [14] G. Yang, Y. Liu, M. Jin, and H. Liu, "A robust and adaptive control method for flexible-joint manipulator capturing a tumbling satellite," *IEEE Access*, vol. 7, pp. 159971-159985, 2019.
- [15] H. Ma, H. Li, H. Ren, and Q. Zhou, "Adaptive fuzzy control for a single-link flexible-joint robotic manipulator with output constraint," in *7th International Conference on Information, Cybernetics, and Computational Social Systems*, 2020, pp. 46-51.
- [16] J. Tavoosi and F. Mohammadi, "A new type-II fuzzy system for flexible-joint robot arm control," in *6th International Conference on Control, Instrumentation and Automation*, 2019, pp. 1-4.
- [17] X. Cheng, H. Liu, and W. Lu, "Chattering-suppressed sliding mode control for flexible-joint robot manipulators," *Actuators*, vol. 10, no. 11, p. 288, 2021.
- [18] S. zaare, M. R. Soltanpour, and M. Moattari, "Voltage based sliding mode control of flexible joint robot manipulators in presence of uncertainties," *Robotics and Autonomous Systems*, vol. 118, pp. 204-219, 2019.
- [19] K. Rsetam, Z. Cao, and Z. Man, "Hierarchical sliding mode control applied to a single-link flexible joint robot manipulator," in *International Conference on Advanced Mechatronic Systems*, 2016, pp. 476-481.
- [20] W. He, Z. Yan, Y. Sun, Y. Ou, and C. Sun, "Neural-learning-based control for a constrained robotic manipulator with flexible joints," *IEEE Transactions on Neural Networks and Learning Systems*, vol. 29, pp. 5993-6003, 2018.
- [21] X. Liu, C. Yang, Z. Chen, M. Wang, and C.-Y. Su, "Neuro-adaptive observer based control of flexible joint robot," *Neurocomputing*, vol. 275, pp. 73-82, 2018.
- [22] M. B. A. Jabali and M. H. Kazemi, "Uncertain polytopic LPV modelling of robot manipulators and trajectory tracking," *International Journal of Control, Automation and Systems*, vol. 15, no. 2, pp. 883-891, 2017/04/01 2017, doi: 10.1007/s12555-015-1432-1.
- [23] A. Fazli and M. H. Kazemi, "Manipulator Dynamic Nonlinearity Approximation Based on Polytopic LPV Modeling for Robot Tracking Control Problem," *Iranian Journal of Science and Technology, Transactions of Electrical Engineering*, vol. 46, no. 2, pp. 537-547, 2022/06/01 2022, doi: 10.1007/s40998-021-00477-y.

[24] H. S. Ali, M. Darouach, L. Boutat-Baddas, and Y. Becis-Aubry, “ \mathcal{H}^∞ state feedback LPV control of a SCARA robot,” in 2007 European Control Conference (ECC), 2-5 July 2007 2007, pp. 4222-4227, doi: 10.23919/ECC.2007.7068605.

[25] A. GZ, System analysis, modeling and control with

Polytopic Linear Models. Universiteitsdrukkerij TU Eindhoven, Eindhoven, The Netherlands, 2003.

[26] O. Nelles, Nonlinear system identification from classical approaches to neural networks and fuzzy models. Springer Nature, 2020.

HOW TO CITE THIS ARTICLE

R. Rajabi, F. Jahangiri, Polytopic Linear Models-Based Output Tracking Control of a Single-Link Flexible Joint Robot Manipulator, AUT J. Model. Simul., 54(1) (2022) 45-58.

DOI: [10.22060/miscj.2022.21076.5270](https://doi.org/10.22060/miscj.2022.21076.5270)



